

Fine Structure of the Gamow-Teller Resonance in ^{90}Nb and Level Density of 1^+ States

Y. Kalmykov,¹ T. Adachi,² G. P. A. Berg,³ H. Fujita,^{2,4,5} K. Fujita,³ Y. Fujita,² K. Hatanaka,³ J. Kamiya,³ K. Nakanishi,³ P. von Neumann-Cosel,^{1,*} V. Yu. Ponomarev,^{1,†} A. Richter,¹ N. Sakamoto,³ Y. Sakemi,³ A. Shevchenko,¹ Y. Shimbara,² Y. Shimizu,³ F. D. Smit,⁵ T. Wakasa,³ J. Wambach,¹ and M. Yosoi⁶

¹*Institut für Kernphysik, Technische Universität Darmstadt, D-64289 Darmstadt, Germany*

²*Department of Physics, Osaka University, Toyonaka, Osaka 560-0043, Japan*

³*Research Center for Nuclear Physics, Osaka University, Ibaraki, Osaka 567-0047, Japan*

⁴*School of Physics, University of the Witwatersrand, Johannesburg 2050, South Africa*

⁵*iThemba LABS, P.O. Box 722, Somerset West 7129, South Africa*

⁶*Department of Physics, Kyoto University, Kyoto 606-8502, Japan*

(Received 30 May 2005; published 6 January 2006)

The fine structure of the Gamow-Teller resonance in a medium-heavy nucleus is observed for the first time in a high-resolution $^{90}\text{Zr}(^3\text{He}, t)^{90}\text{Nb}$ experiment at the Research Center for Nuclear Physics, Osaka. Using a novel wavelet analysis technique, it is possible to extract characteristic energy scales and to quantify their relative importance for the generation of the fine structure. This method combined with the selectivity of the reaction permits an extraction of the level density of 1^+ states in ^{90}Nb .

DOI: 10.1103/PhysRevLett.96.012502

PACS numbers: 24.30.Cz, 21.10.Ma, 25.55.Kr, 27.60.+j

Giant resonances are elementary excitations modes of nuclei. Since they dominate the nuclear response at low energies and low momentum transfer, their experimental and theoretical investigation constitutes a central topic in nuclear physics [1]. While some of the basic features such as centroid energies and collectivity (in terms of sum rules) have been reasonably well understood in microscopic models, no coherent description of the widths has been achieved so far. In heavy nuclei, the doorway-state model provides a widely accepted (but experimentally hardly tested) explanation of the dominant damping mechanism to result from a coupling hierarchy of the initially excited one-particle one-hole ($1p1h$) states to two-particle two-hole ($2p2h$) and finally to $n\bar{p}nh$ states, leading to internal mixing [2]. A recent high-resolution study of the isoscalar giant quadrupole resonance (ISGQR) over a wide mass range provided a new experimental access to this problem [3]. The data systematically exhibited fine structure in the ISGQR energy region from which characteristic energy scales could be extracted with a novel method based on wavelet analysis techniques. With the aid of microscopic models, these characteristic scales were shown to result from the first step of the coupling hierarchy described above.

These important results immediately raise further questions: Is fine structure also found in other collective modes? If so, does it arise from the same mechanism? Can one quantify the relevance of certain scales for the fine structure? The present work addresses these problems by a study of the Gamow-Teller resonance (GTR), i.e., a spin-isospin flip mode in the medium-heavy nucleus ^{90}Nb . Generally, spin-isospin resonances retain more of the single-particle character due to the initial $1p1h$ excitations or, in other words, show less collectivity than electric resonances like the isovector giant dipole resonance

(IVGDR) or the ISGQR. In this Letter, it is demonstrated that the fine structure and corresponding scales are indeed also present in the GTR and, therefore, seem to be a common feature of different classes of resonances. A new method utilizing discrete wavelet transforms (DWT) is presented which provides a direct measure of the importance of the scales generating the fine structure. Moreover, the DWT analysis can be used for a nearly model-independent extraction of level densities. Such data have an important application as a test of level-density models used, e.g., in nucleosynthesis network calculations [4].

In order to search for the fine structure of the GTR, the $^{90}\text{Zr}(^3\text{He}, t)^{90}\text{Nb}$ reaction was investigated at the Research Center for Nuclear Physics (RCNP), Osaka University, Japan using a 140 MeV/nucleon ^3He beam with currents of 10–40 nA. Data were taken with an isotopically enriched (99.4% ^{90}Zr) target with an areal density of 2 mg/cm². Outgoing tritons were detected with the Grand Raiden spectrometer placed at 0° , covering an angle range $\Theta = 0^\circ \simeq 6^\circ$ divided into four bins for further analysis. At scattering angles close to 0° , the selectivity to GT transitions is significantly enhanced. Using lateral and angular dispersion matching, efficiently realized by the “faint beam” method [5], a very good energy resolution, $\Delta E \simeq 50$ keV full width at half maximum, and an angular resolution $\Delta\Theta \simeq 0.3^\circ$ were achieved, permitting detection of the fine structure and identification of GT transitions from the angular distributions of the $(^3\text{He}, t)$ cross sections. Details of the experimental methods are described, e.g., in Ref. [6] and the data analysis in Ref. [7]. The resulting spectrum, shown in Fig. 1(a), is dominated by a prominent GT transition to a 1^+ state at low energies and the excitation of the 0^+ isobaric analog state (IAS) to the ^{90}Zr ground state. A zoom on the GTR region is presented in Fig. 1(b). Pronounced fluctuations are visible which extend to exci-

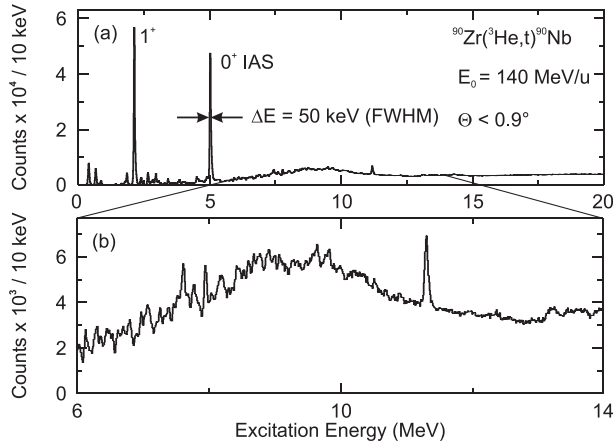


FIG. 1. (a) Spectrum of the $^{90}\text{Zr}(^3\text{He}, t)^{90}\text{Nb}$ reaction at $E_0 = 140 \text{ MeV/u}$ and $\Theta < 0.9^\circ$. (b) Zoom on the GTR region. The prominent peak at $E_x \approx 12 \text{ MeV}$ stems from the ^{12}B ground state excited in the $^{12}\text{C}(^3\text{He}, t)$ background reaction.

tation energies $E_x \approx 14 \text{ MeV}$. Thus, the fine structure phenomenon is also observed for a spin-isospin resonance in a medium-heavy nucleus.

For an extraction of characteristic scales, a wavelet analysis adopted from signal processing theory is used. This technique—with applications in many areas of physics—permits a separation of generic and nongeneric features of the spectrum and the extraction of information in the presence of noise [8]. By folding the original spectrum $\sigma(E)$ with a chosen wavelet function Ψ , coefficients

$$C(E_x, \delta E) = \frac{1}{\sqrt{\delta E}} \int \sigma(E) \Psi\left(\frac{E_x - E}{\delta E}\right) dE \quad (1)$$

are obtained. The parameters (excitation energy E_x and scale δE) can be varied continuously or in discrete steps $\delta E = 2^j$, $E_x = k\delta E$, $j, k = 1, 2, 3, \dots$, corresponding to continuous (CWT) or discrete (DWT) wavelet transforms, respectively. All calculations were performed with the Matlab Wavelet Toolbox [9].

The results of the CWT (performed with a Morlet wavelet as described in Ref. [3]) are displayed in Fig. 2(a) for $\Theta < 0.9^\circ$. The two-dimensional correlation of the absolute values of the wavelet coefficients is shown in the lower-right panel. Scales are identified as maxima extending across the region of the GTR bump at characteristic δE values. A projection on the vertical axis (lower-left panel) allows one to extract values of 50, 80, 300, 950, and 2600 keV. The smallest one visible as a shoulder just below the 80 keV scale results from the experimental resolution, and the largest one (not shown) reflects just the total width of the resonance. The same scales are independently found for the other angular bins.

A corresponding analysis of the GTR with a microscopic quasiparticle-phonon model (QPM) calculation [10] including $2p2h$ configurations is presented in Fig. 2(b). It

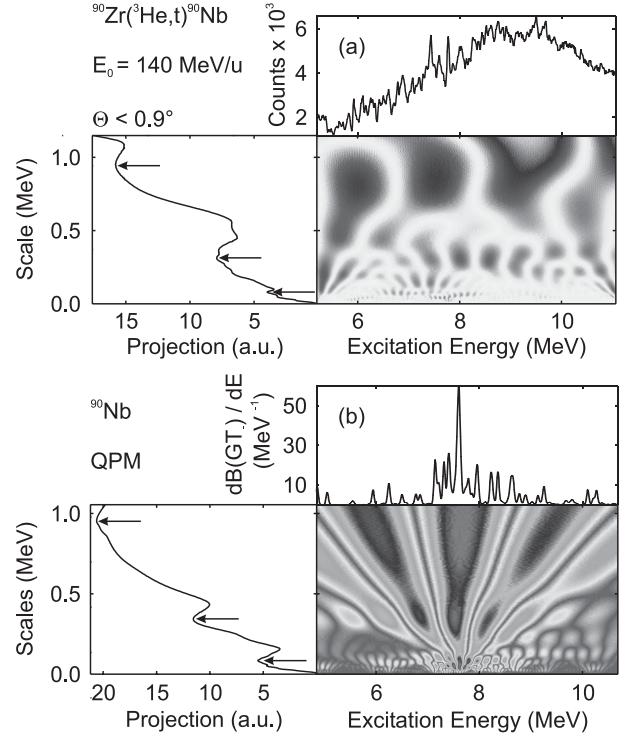


FIG. 2. (a) Continuous wavelet transform analysis of the spectrum of the $^{90}\text{Zr}(^3\text{He}, t)^{90}\text{Nb}$ reaction (upper panel) and absolute values of the wavelet coefficients, Eq. (1), as a function of excitation energy and scale, and their projection on the scale axis (lower panel). (b) Same as (a) but for the GT strength distribution in ^{90}Nb calculated with the QPM.

confirms that the scales arise from the coupling of $1p1h$ to $2p2h$ states since no scales emerge in a pure $1p1h$ calculation. The scales extracted from the QPM (100, 380, 950, and 1600 keV) are in fairly good agreement with experiment except for the total width, which is underestimated. This may result from a yet too small model space omitting the coupling to $n\text{pnh}$ ($n \geq 3$) states and/or the neglect of the continuum.

In the next step, the relevance of the extracted scales for the creation of the fine structure is tested by a discrete wavelet transform analysis which allows one to reassemble the original signal from the wavelet coefficients. The reconstruction is exact if the wavelet functions form an orthogonal basis. Obviously, this condition is never fulfilled in the CWT analysis. However, the choice of scales and energies based on powers of two in the DWT makes the reconstruction possible. This scheme is known as two-channel subband coding in signal processing and can be interpreted as the application of low-pass (large scales δE) and high-pass (small δE) filters on the spectrum separating it into a so-called approximation A and detail D , respectively. Starting at the smallest possible scale ($j = 1$), one gets $\sigma(E) = A_1 + D_1$. In the second step, A_1 is decomposed into A_2 and D_2 , and so forth. While the ability of this method for a precise determination of characteristic scales

is limited, it allows one to explicitly test the contributions of different scale regions.

An application to the data is presented in Fig. 3. A BIOR3.9 [8] instead of a Morlet wavelet function is used here because it provides an orthogonal basis required for the DWT analysis. One finds that certain intervals (e.g., D_3, D_4) are larger in magnitude than others (e.g., D_1, D_2). A reconstruction of the original spectrum choosing different sets of details is presented in Fig. 4, where the reconstructed spectra are displayed in the upper part and the differences to the original spectrum in the lower part. The left-hand side takes into account D_3 – D_6 , whereas the remaining ones are used on the right-hand side. All significant fluctuations are reproduced in the first case, while only the global shape of the resonance, basically determined by A_8 , is observed in the second case.

Another useful feature of wavelet functions can be used for background determination. Every wavelet function can be characterized by the number of its vanishing moments

$$\int E^n \Psi(E) dE = 0 \quad \text{with } n = 0, 1, \dots, m. \quad (2)$$

For example, the BIOR3.9 wavelet function has $m = 2$. Therefore, any background in the spectrum, whether instrumental or due to quasifree charge-exchange reactions or $L > 0$ multipole strength, does not contribute to the wavelet coefficients if it can be approximated by a polynomial of second order. This allows a nearly model-independent extraction of another important information hidden in the fine structure, viz. the mean level spacing $\langle D \rangle$, respectively, its inverse $\rho = \langle D \rangle^{-1}$, the level density. Because of the selectivity of the ($^3\text{He}, t$) reaction under 0° , the present experiment measures the density of $J^\pi = 1^+$ states in ^{90}Nb .

In a spectral region where the mean level spacing $\langle D \rangle$ is smaller than the experimental energy resolution but larger

than the mean level width $\langle \Gamma \rangle$, the level spacing can be determined by means of an autocorrelation function analysis. The method is described in detail elsewhere [11]. Briefly, a so-called stationary spectrum is prepared from the original data which contains only the local fluctuations (i.e., all gross structures are removed). Its autocorrelation function $C(\epsilon)$ can be approximated by the following expression [11]:

$$C(\epsilon) - 1 = \frac{\alpha \langle D \rangle}{2\sigma\sqrt{\pi}} \times f(\epsilon, \sigma). \quad (3)$$

Here $f(\epsilon, \sigma)$ denotes a function depending on properties of the experimental spectrum only. For a class of states with given spin and parity, α is the sum of the normalized variances of the spacing and transition width distributions assumed to be of Wigner and Porter-Thomas type, respectively. However, all applications of this method so far required additional assumptions, either about the exact shape of the background or about the level spacings, which had to be taken from models (such as the ones discussed below).

In the present case, an extraction of the level density of the 1^+ states is possible without prior knowledge of the background based on the DWT decomposition (Fig. 3). Because of the sufficient number of vanishing moments, the approximation corresponds to the background at some stage of the DWT decomposition and does not carry anymore information on the fine structure. This stage is reached when the largest characteristic scale (i.e., the width of the resonance) is present in the approximation. As seen in Fig. 4, the broad structure of the GTR is given by A_8 , so that A_9 can be considered as a background shape to the spectrum. Indeed, it is well approximated by a quadratic function as required for the application of Eq. (2). The procedure is model-independent except for a vertical shift

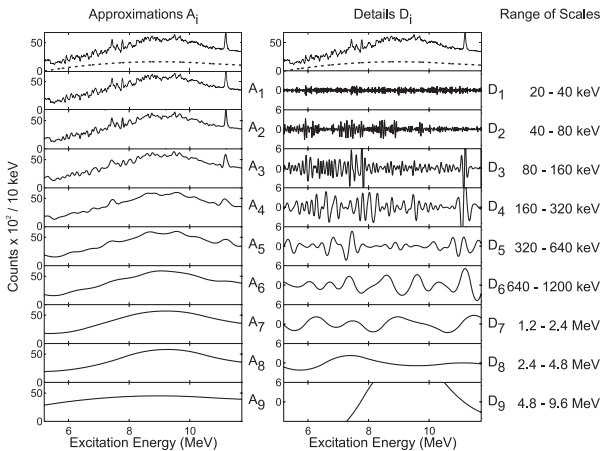


FIG. 3. Discrete wavelet transform decomposition of the $^{90}\text{Zr}(^3\text{He}, t)^{90}\text{Nb}$ spectrum of Fig. 1 into approximations A_i and details D_i . The dashed line in the total spectrum represents the deduced background (see text).

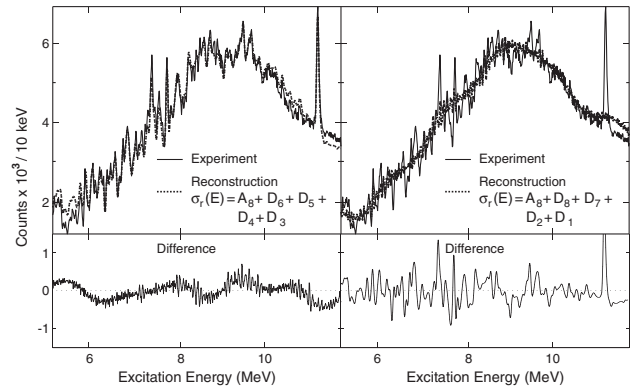


FIG. 4. Top: Reconstruction (dotted line) of the spectrum plotted in Fig. 1 (solid line) including either the scale ranges predicted to be important (left-hand side) or unimportant (right-hand side) in the DWT analysis. Bottom: Differences to the original spectrum.

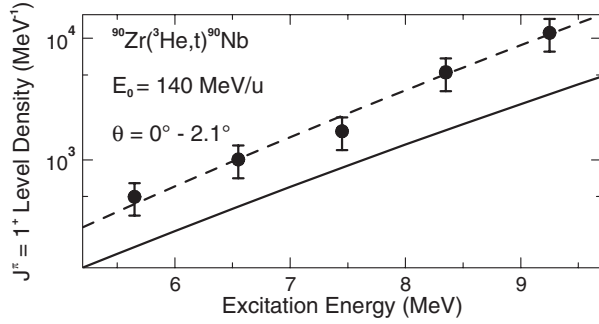


FIG. 5. Level density for 1^+ states in ^{90}Nb obtained from the $^{90}\text{Zr}(^3\text{He}, t)^{90}\text{Nb}$ measurement. Dashed line: Backshifted Fermi gas model [12]. Solid line: Hartree-Fock-BCS calculations [13].

of A_0 in order to satisfy the observation that the spectrum is background-free below the IAS.

The analysis is repeated independently for all four analyzed angle bins. Since the background shows a different angular dependence than the GT strength, the requirement of a constant level density in all spectra further constrains the analysis and confirms the validity of the chosen background shape. This method also allows one to draw certain conclusions on the physical nature of the background [7], which are, however, beyond the scope of the present work. Results in the region $E_x = 5.5\text{--}9.5$ MeV in ^{90}Nb are shown in Fig. 5 along with the predictions of two models commonly used in applications for astrophysical network calculations [4]. A global parametrization of the backshifted Fermi gas model [12] reveals good agreement with the data, while microscopic Hartree-Fock-BCS calculations [13] provide the correct energy dependence but are about a factor of 2 too small.

In summary, due to the excellent resolution achieved and the high selectivity of the $(^3\text{He}, t)$ reaction to Gamow-Teller transitions, the present experiment allows one to unravel for the first time the fine structure of the GTR in a medium-heavy nucleus. Thus, fine structure of giant resonances in nuclei seems to be a global phenomenon not only for electric resonances such as the ISGQR but also in spin-isospin flip modes. This view is further supported by indications of fine structure in high-resolution (e, e') [14,15] and (p, γ) [16] studies of the IVGDR and in $M2$ resonances [17]. A CWT analysis [3] permits one to extract scales characterizing the fine structure of the GTR in ^{90}Nb . By comparison, with a QPM calculation one can connect the appearance of the fine structure in the GTR to the mixing of $1p1h$ doorway states with $2p2h$ states, suggesting dominance of the spreading width for the GTR decay as found for the ISGQR. However, direct decay contributions from the GTR in ^{90}Nb may be as large as 20% [18]. In order to evaluate their influence, an extension of the microscopic models to include continuum coupling is called for.

An essential extension of the wavelet method is presented by means of a DWT analysis providing a quantita-

tative measure of the relevance of fluctuations on given scales for the generation of the fine structure. The DWT also provides a nearly model-independent method of background determination. This together with the sensitivity of the reaction enabled the extraction of the level density of 1^+ states in ^{90}Nb in the region of GTR serving, e.g., as an important test of level-density models used in astrophysical network calculations. So far, these models neglect a possible parity dependence [19]. Applications of this new method to the fp -shell mass region (of prime interest in astrophysics [4]) would be important, where a significant parity dependence is predicted [20] but questioned by recent experiments [21].

The experiment was performed at RCNP, Osaka University, under the experimental program E185. We are grateful to the accelerator group for providing a high-quality ^3He beam. This work was supported by the DFG under Contracts No. SFB 634 and No. 446 JAP-113/267/0-1.

*Electronic address: vnc@ikp.tu-darmstadt.de

†Permanent address: BLTP, JINR, Dubna, Russia.

- [1] M. N. Harakeh and A. van der Woude, *Giant Resonances: Fundamental High-Frequency Modes of Nuclear Excitation* (Oxford University, Oxford, 2000).
- [2] P. F. Bortignon, A. Bracco, and R. A. Broglia, *Giant Resonances: Nuclear Structure at Finite Temperature* (Harwood Academic, Amsterdam, 1998).
- [3] A. Shevchenko *et al.*, Phys. Rev. Lett. **93**, 122501 (2004).
- [4] K. Langanke and M. Wiescher, Rep. Prog. Phys. **64**, 1657 (2001).
- [5] H. Fujita *et al.*, Nucl. Instrum. Methods Phys. Res., Sect. A **484**, 17 (2002).
- [6] Y. Fujita *et al.*, Phys. Rev. C **70**, 054311 (2004).
- [7] Y. Kalmykov, Ph.D. thesis, Technische Universität Darmstadt, 2004.
- [8] *Wavelets in Physics*, edited by J. C. van den Berg (Cambridge University Press, Cambridge, England, 1999).
- [9] <http://www.mathworks.com/products/wavelet/>
- [10] V. G. Soloviev, *Theory of Atomic Nuclei: Quasiparticles and Phonons* (Institute of Physics, Bristol, 1992).
- [11] P. G. Hansen, B. Jonson, and A. Richter, Nucl. Phys. **A518**, 13 (1990).
- [12] T. Rauscher, F.-K. Thielemann, and K.-L. Kratz, Phys. Rev. C **56**, 1613 (1997).
- [13] P. Demetriou and S. Goriely, Nucl. Phys. **A695**, 95 (2001).
- [14] S. Strauch *et al.*, Phys. Rev. Lett. **85**, 2913 (2000).
- [15] H. Diesener *et al.*, Nucl. Phys. **A696**, 272 (2001).
- [16] R. Bergere, Lect. Notes Phys. **61**, 1 (1977).
- [17] P. von Neumann-Cosel *et al.*, Phys. Rev. Lett. **82**, 1105 (1999).
- [18] J. Jänecke *et al.*, Nucl. Phys. **A687**, 270c (2001).
- [19] D. Mocalj *et al.*, Nucl. Phys. **A718**, 650c (2003).
- [20] Y. Alhassid *et al.*, Phys. Rev. Lett. **84**, 4313 (2000).
- [21] S. J. Lokitz, G. E. Mitchell, and J. F. Shriner, Jr., Phys. Lett. B **599**, 223 (2004).